Influence of cellular structure in catalytic reactors for H2 production: Application to improvement of methanol steam reformer by the addition of a copper foam

Stephanie Catillon, Catherine Louis, Frédéric Topin, Jérôme Vicente, Robert Rouget

Influence of cellular structure in catalytic reactors for H_2 production: Application to improvement of methanol steam reformer by the addition of a copper foam

S. Catillon[a, c], C. Louis[a], F. Topin[b], J. Vicente[b], R. Rouget[c]

[a]L R S, UMR 7609 CNRS, UPMC, 4 place Jussieu, 75252 Paris cedex 05,

[b]IUSTI, UMR 6595 CNRS, EPUM, 5 Rue E. Fermi, 13453 Marseille cedex 13

[c]S. C. P. S., 85-93 Boulevard Alsace-Lorraine, 93115 Rosny-sous-Bois cedex

Abstract-- **An experimental set-up was designed to simulate an evaporator and analyze the heat transfer and two-phase flow behavior on n-pentane in the presence and in the absence of copper foam. In monophasic conditions, the heat transfer coefficient was improved by two orders of magnitude by the presence of metallic foam with only a limited increase of pressure drop. In biphasic condition, the study of convective boiling regime also showed significant heat transfer enhancement with very low-pressure drop. Specific morphological tools including 3D visualization and reconstruction were developed to explore the texture of metal foams using X-ray micro-tomography. The catalytic properties for methanol steam reforming of a foam-based Cu-Zn/Al_2O_3, synthesized in situ in three steps, reveal a hydrogen production five times greater than for commercial catalyst, i.e., 9.5 instead of 2.4 L_{H2}/(h.g) for a conversion of 78%.**

***Index Terms*— metal foam, H2 production, reforming, evaporator, morphology.**

I. Introduction

One of the important issues for the catalytic reformer units, which supply hydrogen to fuel cells on board of electric vehicles is the reduction of their volume. Those of the evaporator and of the catalytic reactor are related to problems of heat transfer. For instance, the reaction of steam reforming of methanol, catalysed by Cu/ZnO type catalyst is an endothermic process.

$CH_3OH + H_2O \rightarrow CO_2 + 3\ H_2\ ; \Delta H^0 = +\ 50$ KJ/mol

A promising way to solve these problems is to use thermal conductive structured supports with high porosity, such as metallic foam. The goal of this study was therefore to investigate the heat transfer properties of metallic foams inserted in the evaporator and in the catalytic reactor. The insertion of metallic foam in the evaporator should increase the methanol vaporization velocity and improve the thermal exchange between the reactant feed mixture and the reactor wall. The influence of the metallic foam as catalytic support on the steam reforming reaction was studied, on the one hand, by inserting copper foam with commercial

powder catalyst, and on the other hand by testing a new type of Cu-Zn/Al_2O_3 catalyst supported on metallic foam, which was prepared *in situ*.

II. EXPERIMENTAL

A. *Fabrication and characteristics of the copper foam*

The fabrication of metallic foam at an industrial scale was developed by S.C.P.S. [1]. It consists of the metallization of copper by electrolysis onto conductive polyurethane foam followed by a thermal treatment to remove the organic material and to anneal the copper. In this study, we used a 45 PPI (number of pores per linear inch) grade copper foam (porosity 95%). This corresponds to an average pore size of about 0.6 mm. The foam is manufactured as plates, 3 to 7 mm thick (Fig. 1).

B. *Experimental set-up for the evaporator*

The boiling mechanisms in copper foam and the evaluation of the impact of the solid matrix on flow and heat transfer phenomena were studied in an experimental set-up simulating an evaporator. It consisted of a rectangular channel (10x50x200 mm) that contained the 45 PPI grade copper foam. A liquid (i.e., n-pentane, low toxicity, low boiling point: 36 °C at atmospheric pressure, low phase change enthalpy) flowed through the porous media vertically from the bottom to the top. The channel was instrumented with 40 thermocouples and 15 pressure sensors.

C. *Catalyst preparation*

Methanol steam reforming was studied with Cu-Zn/Al_2O_3-based catalysts. The copper foam was used as a support for this catalyst, which was prepared *in situ* on the foam in three steps: copper foam was first submitted to a thermal treatment in air at 400°C for 3 min and to chemical treatments to increase the roughness of the metallic surface and favor the adhesion of the alumina washcoat performed in the second step. The copper foam was immersed for ~5 seconds in the colloidal solution containing the alumina binder (0.16 g/L of 10 wt % of acidified α-Al_2O_3 sol, Dispersal P2, Sasol) and the alumina (0.33 g/L of γ-Al_2O_3 powder, PURALOX SBA-200, Sasol). The alumina-coated foam was dried at 100°C for 1h and calcined in air from 25 to 300°C with a heating rate of 1°C/min. The third step consists of the deposition of the active copper-zinc phase, which was carried by deposition-precipitation with urea. The alumina-coated foam was immersed in 500 mL of solution of copper and zinc nitrates (MERCK) (3.8 g/L of $Cu(NO_3)_2.3H_2O$ and 4.7 g/L of $Zn(NO_3)_2.6H_2O$ with a molar ratio Cu:Zn=1) to which urea (urea:(Cu+Zn)= 8, $(NH_2)_2CO$, MERCK)) was added. The mixture was heated at 90°C. This leads to the decomposition of urea, so to the gradual basification of the solution (the pH increases from 3.8 to 5.8 within two hours), and to the precipitation of copper and zinc hydroxides onto alumina. Then, the foam-based Cu-Zn/Al_2O_3 catalyst, called foam catalyst in the following, was dried at 90°C for 30 min. The color of the sample was blue-green. The composition of the foam catalyst was 20 wt. % Cu and 9

wt. % Zn. Prior to catalytic reactions; the catalyst was reduced without former calcination, in a 10 vol. % H_2 in Ar flow, from 25 to 400°C with a heating rate of 5°C/min. Two CuO-ZnO-Al_2O_3 commercial catalysts (Süd-Chemie) (60 wt. % of CuO, 30 wt. % of ZnO and 10 wt. % of Al_2O_3) as pellets (6x3 mm, C18-HA) and powder (G-66) were used as reference catalysts.

D. Experimental set-up for the reaction of methanol steam reforming

Methanol steam reforming was carried out in a laboratory reactor (length= 300 mm; Ø= 10 mm, except for powder catalyst test Ø= 21 mm) system under the following conditions: T_R= 220-280°C, a pressure of 3 bars; a liquid feed of H_2O:MeOH= 1.5 vaporized and diluted to N_2 such as the gas feed composition was 15-30 vol.% H_2O, and 10-20 vol.% MeOH. Hourly Space Velocities (HSV) are reported in Table 1. After condensation of liquids (water and methanol) at the outlet of the reactor, dried gases, produced by the reaction (H_2, CO_2, CO) were analyzed by gas chromatography (Perichrom) equipped with columns Porapak Q and molecular sieves, and thermal conductive detector (TCD).

III. RESULTS AND DISCUSSION

A. Heat transfer and fluid flow in the evaporator

We studied the boiling mechanisms in copper foam and evaluated the influence of the solid matrix on flow and heat transfer phenomena. Flow properties (permeabilities, friction factors…) were measured and both viscous and inertial coefficients were deduced (Fig.2).

The inertial effects were always preeminent in contrast with classical porous materials (glass beds…) because of the specific geometric texture of this foam (95 % of porosity). We obtained a permeability K ~1,4 10^{-8} m^2 and an inertial coefficient β/ρ= 1169 m^{-1}. The inertial coefficient was determined with an accuracy of around 5% whereas the permeability could not be evaluated accurately even for low velocities, because the viscous effects represent only a few percent of the pressure losses [2].

The temperature profiles measured in the channel containing the metallic foam and free of foam (“empty”) revealed that the monophasic heat transfer coefficient was improved by two orders of magnitude by the presence of the foam, with a limited pressure drop (less than 1 order of magnitude) (fig. 3).

This corresponds to a heat transfer coefficient comparable to that of fibrous materials [3] but to a pressure drop reduced by one order of magnitude compared to the fibers. The boiling curve (Figure 4) of the heat flux as a function of the wall superheat (ΔT: temperature difference between the wall and the fluid) was measured for two cases (i) the foam welded to the wall and (ii) the foam just inserted in the channel. The onset of boiling starts at very low superheat (ΔT ~0.1 and 1°C, respectively) compared to the “empty” channel whose ΔT is about 10 °C. The heat flux strongly increases when the superheat increases. The fluid velocity has no influence on the heat flux, even at low superheat and very low fluid velocity (10–40 kg $m^{-2}.s^{-1}$). The critical heat flux, for

which the walls dry out (formation of a insulating vapor film on the walls leading to a overheating), was not reached with our set-up, and so, largely exceeds 30 kW.m^2.

Performances of copper foam were compared to other fibrous materials. The boiling curve obtained in the same conditions for bronze sintered fibers, which are known for their high thermal performances [4], is similar to the foam inserted at low superheat (Figure 4). However, when the superheat exceeds 10 °C, the heat flux is far smaller than for the foam. The high performance of the foam is linked to its open structure that permits an easy evacuation of the vapor formed near the wall. This improves the heat transfer and avoids the phenomenon of dry out. Moreover, the pressure drop generated in the foam is 10 times smaller than those in the sintered fibers for the same heat transfer and velocity conditions.

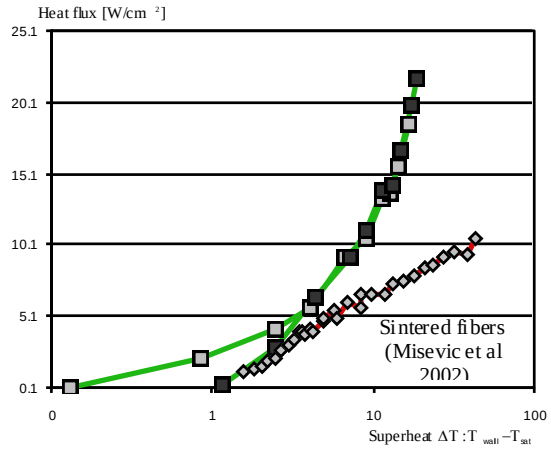

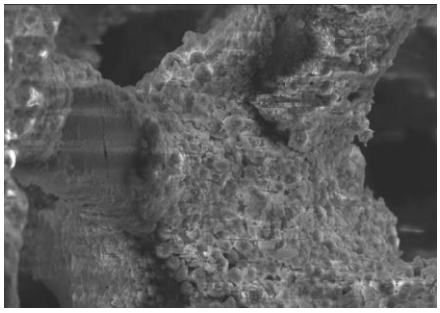

Fig. 5. *View of a strand of the foam catalysts after 24h of steam reforming reaction*

Fig. 4. *Boiling Curve: copper foam compared to sintered bronze fibers. Black squares: inserted; Gray squares: welded; diamond: bronze fibers*

B. Effect of the copper foam on the methanol steam reforming reaction

To evaluate the improvement of the heat transfer due to the copper foam, the catalytic behavior of 10 g of commercial powder G-66 catalyst mechanically mixed to the foam was compared to that of the catalyst alone. The addition of copper foam leads to a decrease of 30°C of the reaction temperature (250 instead of 280 °C) for the same conversion (70%) of methanol into H_2 and the same HSV of 570 h^{-1}. The decrease of the temperature of methanol steam reforming was also observed by Wild and Verhaak [5] in a previous study performed with a commercial catalyst deposited on aluminum foam by washcoat

.

Table 1: Comparison of the catalytic properties for methanol steam reforming of the foam catalyst with commercial catalysts

	Cu-Zn/Al$_2$O$_3$ catalyst			
	Powder G-66	*Pellets C-18HA*		*Foam catalyst*
Catalyst weight (g)	10	6	4.5	1.16
Catalytic bed volume (L)	0.02	0.0125	0.009	0.009
Space velocity (h^{-1})	570	900	1250	1250
Conversion (%)	70	96	78	77
H_2 produced (L/(h.g))	1	2.3	2.4	9.5
H_2 produced (L/(h.cm^3))	0.5	1.16	1.18	1.17

Then, the catalytic performances of the foam-based Cu-Zn/Al_2O_3 catalyst prepared *in situ* were compared with those of the commercial pellets C-18HA catalyst (which is more active than powder G-66, see Table 2). The foam catalyst reveals a high activity for the steam reforming reaction, since the methanol conversion into hydrogen reaches 78 %. Moreover, for the same catalytic bed volume of 0.009 L, the hydrogen production was five times greater for the foam catalyst than for than the commercial C-18HA catalyst (Table 1) ; however, the volume of hydrogen produced expressed per volume unit of catalyst is the same for both the pellets and foam catalysts. The study of the improvement of the reformer compactness using foam-based catalyst bed is in progress in the case of a reforming unit prototype design of a 1kW power.

It is noteworthy that the MEB micrographs of the foam catalyst after reaction reveal that the adhesion of the catalyst on the metal foam remains good after 24 hours of reaction.

IV. MORPHOLOGY OF THE COPPER FOAM

Data of the literature reported that metal foams of apparently similar geometry exhibit extremely different transport properties. So, the choice of the foams for a given application (boiler, vapo-reformer…) is crucial, and can be done if it is possible to correlate their microscopic structure to the transport properties. The control of the texture of porous materials used for the optimization of compact and multipurpose exchangers of heat represents a significant technological stake. This requires that the morphological characterization of the foam structure can be performed, and this is a difficult issue.

A first study [6] showed up the feasibility of the 3D rebuilding of a metal foam (10 PPI) starting from serial cuts obtained by Computed X-ray tomography of 150µm resolution. Nevertheless, the 3D image is insufficient alone for characterizing the geometry of the foam.

We characterized both pore space and solid matrix from a geometric point of view as these two parts may have independent geometric characteristics. These latter impacts on various properties (e.g heat conductivity is linked mainly to matrix structure, flow laws are governed by pore shape).

We present here several structural indicators which allow us to differentiate the shape of three-dimensional structures (pore/matrix).

A. Segmentation/binarisation

The segmentation consists in extracting, from 2D or 3D images, points or areas which are then used for visualization, measurement or morphometry. The method consists in decomposing the histogram of voxel density on a basis of function, each one pertaining to a different class in the image. This technique is adapted to our well contrasted pictures of a medium containing only two phases (solid/pore). For each cut, an optimal threshold based on the density histogram was calculated. The binarisation (pore/solid) thus gives us the direct 3D rebuilding of the foam in terms of empty or solid voxels.

B. Pores size distribution

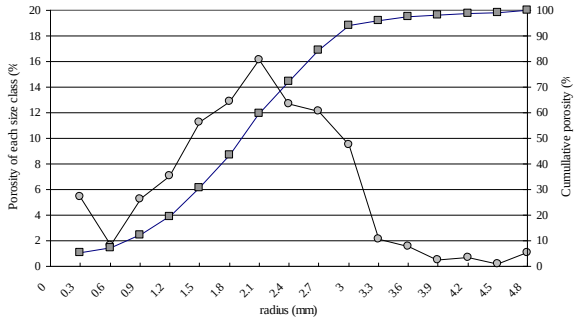

Fig. 6. *Porosimetric analysis : Aperture diameter distribution (circles) and its cumulative repartition (squares). 10 ppi metallic foam sample.*

C. Tortuosity

The tortuosity of a medium was for the first time defined by Carman [8] and given, in a particular direction, like the square of the ratio of the average effective distance traversed by the fluid at the Euclidean distance between 2 sections. As we reconstruct the shape of the solid matrix it is interesting to define a geometrical tortuosity for each phase. This one is defined, for a couple of points contained in the same phase and connected according to :

$$\tau_g(p_1, p_2) = \left[\frac{L_{\min}(p_1, p_2)}{\|p_1 - p_2\|} \right]^2 \qquad (2)$$

with L_{min}, the lenght of the shortest way joining p_1 to p_2.

To determine the geodesic distance between two points we use

a Fast Marching Method. FMM [9,10] are mainly used for the construction of geodesic on surfaces, or calculation of the optimal ways circumventing of the obstacles.

The FMM constitutes the base of several indicator measurements and structural schematization tool (squelettisation, branching detection,..).

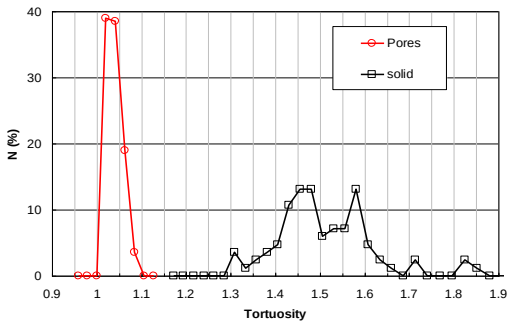

Fig. 7. *Distribution of tortuosity of both solid and pore calculated between two parallel plane distant from 30mm. (copper sample 10 PPI)*

D. Tesselation : specific surfaces, porosity

We use the "Marching cubes" algorithm [11] to approximate the interface between the solid matrix and the pores by a whole of polygonal facets (Isodensity surface) with a better precision than the original 3D binary image.

The reconstruction of the dividing surface between solid and pore allows the visualization of the 3D data (figure 6 & 9). This function is essential to validate the 3D rebuilding, as well as the various techniques of segmentation used for the recognition of the structuring elements of the metallic foam (segments, nodes, cells,..). The reconstructed surface is made of a regular triangularisation, of which we check connectivity of edges, and which does not present holes. We can then carry out the direct calculation of surfaces and specific volumes of each phase of the foam (cf. §E). We also export the surface grid of the solid matrix (or poral space) as toward research or commercial computer codes to simulate the transfers in these mediums [12].

E. Schematic analysis: solid and pores network

The extraction and the automatic recognition of the structuring elements constitute the base of the geometrical description. Indeed, the identification and the three-dimensional localization of nodes (segment junctions), segment and the connectivity table allow us to access the geometrical characteristics. We focus on the determination of connectivity of both solid matrix and pores. The network reconstruction open access to statistic treatment of : Segment length, orientation, as well as highlighting preferentially directed planes.

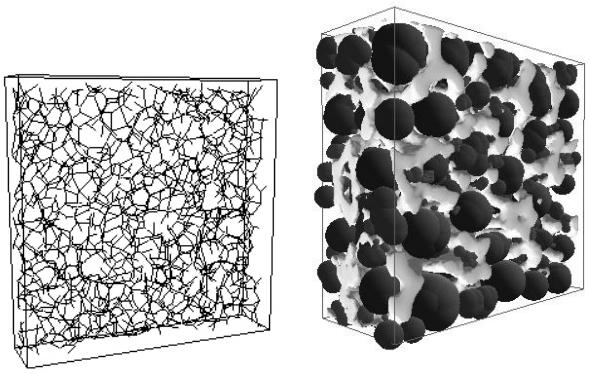

a) b)

Fig. 8. *a) Structural schematization of solid phase (Network of interconnected segment b) Network model of pores constituted of maximal spheres included into the poral space and connected by the centerlines. The solid phase is represented in light grey.*

The detection of the junctions of the solid matrix enables us to cut out it in structuring elements (segment, nodes) from which we build a idealized network of linear segments.

The method of node detection is based on the propagation of a wave front inside the solid matrix and on the detection of the locations where this front divides itself. Indeed, the points where 2 (or more) fronts collapse could also been node if they are connected to at least 3 other nodes. In order to obtain accurate detection a centerline construction, using FMM methods [13], is applied to the solid matrix and the propagation is made in the resulting centerline.

In a similar way, the pore space is constituted of interconnected cells, thus the same methodology was applied, and the poral space is decomposed in a network of maximal spheres (Fig. 8).

F. 3D measurements

We present the specific surface per unit of volume of solid phase and the apparent one (per unit of sample volume). The porosity obtained here is lower than the one obtained by weighing because of the weak resolution of the tomography that does not enable distinguishing empty spaces inside the solid. This bias will not exist with higher resolutions images.

For each phase, we measure the geometrical tortuosity between two parallel planes (z0, z1) situated at the two extremity of the sample, and distant of 30mm (figure 5). Each value is obtained for couple of points {(x y z0), (x y z1)} belonging to the same phase and placed at the same position in each plane.

The figure 7 shows the distribution of these tortuosities for each phase. The tortuosity distribution of poral space is very narrow and centered on a low values that indicates a very open texture of pores. On the other hand, the tortuosity distribution of the solid phase is rather large, with an average value of 1.52 that highlight the solid matrix is constituted of rather short ligaments of different orientations.

The connectivity is the average number of nodes connected to each node of the solid network. The low value of connectivity (3.38) shows up that the real network is different from the classical idealized matrix which is made of periodic polyhedral cells (connectivity of the periodic network superior to 4).

Table 2: X-Ray tomography analysis of a 10 PPI grade copper foam. Sample size: 30x30x6.3mm, resolution 0.15mm.

	Volume (mm^3)	*Specific surface /vol. solid (m^{-1})*	*Specific surface (apparent) (m^{-1})*
Sample	5557.167	5375	941
	Volume (mm^3)	*Porosity (%)*	*Tortuosity*
Pore	4583.707	82.5	1.03
Solid	973.46	17.5	1.52
	Ligament length (mm)		*Connectivity*
Solid network	1.17		3.38

G. Conclusions

We produced a 3d morphological analysis tool starting from 2d serials cut serial images obtained by X-ray tomography. This tool provides the functions of visualization, geometrical measurements and schematization of idealized network. This whole of complementary functionalities will enable us to proceed to the morphology analysis in correlation with the physical transport properties.

This study illustrates the improvement of both monophasic and biphasic heat transfer given by the use of copper foam in a channel. The superheat at the onset of boiling is reduced and the heat transfer is increased. The flow laws in these materials are dominated by inertial effects, but the pressure drop generated in these materials remains very low. These results show a very strong impact of the foam structure on heat transfer and fluid flow. In the catalytic reformer, the insertion of copper foam with commercial Cu-Zn/Al2O3 catalyst improves the thermal exchange, leading to a decrease of 30°C of the temperature reaction. A new copper foam based Cu-Zn/Al2O3 catalyst, which was prepared by an in situ three steps procedure, shows a methanol conversion of 78 % corresponding to a hydrogen production of 9.5 L/(h.g).

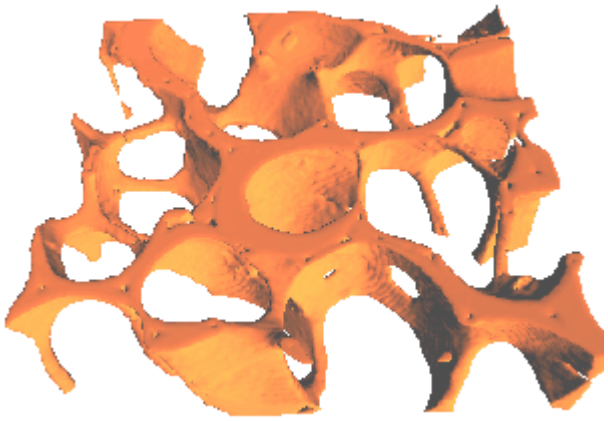

Fig. 9. *3D Vizualisation of reconstructed structure of a foam using High resolution (5 µm) X-ray tomography*..

ACKNOWLEDGMENT

The authors wish to thank Süd-Chemie for providing reference catalysts, and the French Ministry of Research, within the framework of a PACo programme including also the CEA/GRETh as partner.

REFERENCES

[1] SCPS, FR Patents, 1995, 9509547, 1998, 9803375.

[2] B. Madani, F. Topin, L. Tadrist, F. Rigollet ; «Pressure drop in metallic foam : emphasis on flow laws experimental determination» ; Submitted to Journal of porous media; 2004

[3] L. Tadrist, M. Miscevic, O. Rahli and F. Topin «About the Use of Fibrous Materials in Compact Heat Exchangers» ; Experimental Thermal and Fluid Science, vol 28, 2004, pp 193 – 199

[4] M. Miscevic, F. Topin, L. Tadrist, „Convective boiling phenomena in a sintered fibrous channel:Study of thermal non-equilibrium behavior“ ; Journal of Porous Media, Vol 5, N°4, 2002, pp. 229-239

[5] De Wild P.J. and M.J.F.M. Verhaak, 2000, Catal. Today, 60, 3.

[6] S. Catillon, C. Louis, F. Topin, J. Vicente, R. Rouget «Improvement of methanol steam reformer for H2 production by addition of metal foam in both the evaporator and the catalytic reactor»; H2-age : When, Where, Why, Pisa, Mai 2004, Chemical Engineering Transactions, Volume 4, 2004, pp 111-117

[7] J.F. Delerue, E. Perrier, Z. Yu, B. Velde, New algorithms in 3D image analysis and their application to the measurement of a spatialized pore size distribution in soils, Physics and Chem. of the earth, 24-7 (1999), 639-644.

[8] Carman, P.C. Fluid flow through granular bed, Trans. Instn, Chem. Engrs. (London), 15:150—156, 1937.

[9] J.A. Sethian, Level Sets Methods and fast Marching methods, Cambridge Univ. press (1999).

[10] T. Deschamps, L.D. Cohen, Fast extraction of minimal paths in 3D images and applications to virtual endoscopy, Medical Image Analysis 5-4 (2001).

[11] Lorensen W. E, Cline H.E. , Marching Cubes : A High Resolution 3D Surface Construction Algorithm, In SIGGRAPH'87 Proc., 21 (1987), 163-169.

[12] Daurelle J.V., Topin F., Vicente J. «Modélisation des phénomènes de transport dans les mousses métalliques : Influence des contacts pariétaux »; Congrès de la SFT 04, Mai 2004

[13] A.C. Telea, J.J. van Wijk, An Augmented Fast Marching Method for Computing Skeletons and Centerlines, In EG/IEEE VisSym 2002 Proc, ACM Press (2002), 251-260.